AMSI VACATION RESEARCH SCHOLARSHIPS 2019–20

EXPLORE THE MATHEMATICAL SCIENCES THIS SUMMER

Bouncing Balls on Oscillating Tables

Julian Ceddia

Supervised by Dr. Joel C. Miller

La Trobe University

Vacation Research Scholarships are funded jointly by the Department of Education and the Australian Mathematical Sciences Institute.

Abstract

In this research, we examine the period-doubling bifurcations exhibited by the dynamical system of a ball bouncing on a vertically oscillating table. We construct a numerical simulation in MATLAB and an apparatus to experimentally corroborate simulated behaviour. We observed period-doubling bifurcation from 1st order periodic motion, n=1 up to n=16, and verified n=1 and n=2 cases experimentally, with a new kind of apparatus. We also find cases of stable period-3 motion which bifurcate into period-6, and subsequently period-12.

I. Introduction

In 1982, P.J. Holmes was the first to formalise an investigation into the behaviour of a ball bouncing vertically on a sinusoidally oscillating plate [1-2]. Holmes' simplified model contains various assumptions which do not withstand experimental foist [2]; however he opened the door to an area of research that has been a topic of scrutiny for numerous mathematical scientists since. Fig. 1 shows the system, investigated by Holmes and others [1-6], which is the primary focus of this article.

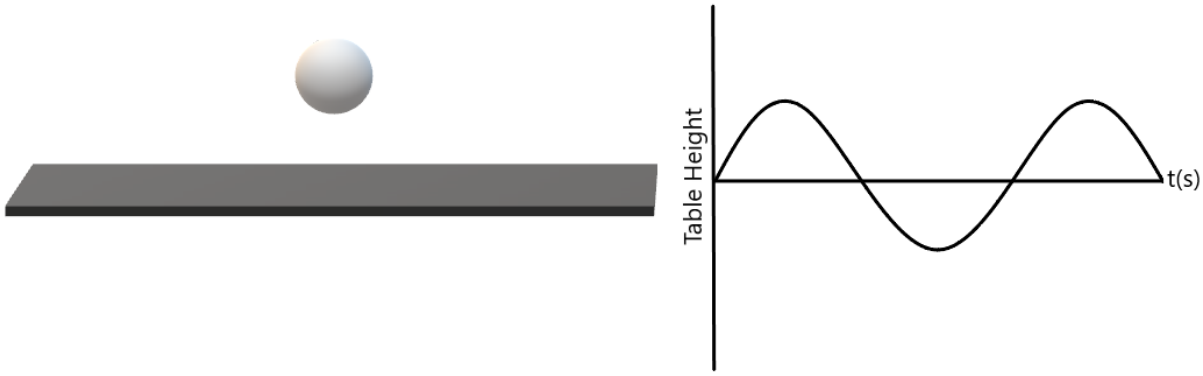

Fig 1 - *A ball, with coefficient of restitution e, bouncing on a rigid, vertically oscillating table.*

There is a surprisingly rich and complex domain of behaviour afforded by this one-dimensional system [1, 3-5]. On one hand, attracting periodic solutions exist such that the motion of the ball approaches n-periodic motion, where n is the number of distinct bounces within a period [1, 3]. On the other, chaotic behaviour abounds when the initial conditions do not permit periodic motion and 'sticking solutions' are non-existent, due to collision duration [6]. In numerical simulations that do not take into account velocity dependant coefficients of restitution, or collision duration, chaos is never observed [3]. In these cases, sticking solutions where the ball bounces an infinite number of times, before locking to the table in a finite time period, are extant. The ball is then launched from a specific point in the table's phase, ultimately resulting in periodic motion [3,6]. Experimentally, the door to chaotic behaviour is always ajar [4-6], due to the role played

by the velocity dependant contact time between the ball and the plate shown by Jiang, Liang, and Zheng in [6], as well as imperfections in the physical system.

In this research, we use a combination of experimental and theoretical tools to explore the system in more detail. The theoretical model presented in this paper ignores the effects of contact duration; we are primarily studying stable periodic solutions, and we assume the table is rigid, such that its motion is undisturbed by the bouncing ball. With a model built on these key assumptions, we explore the parameter space of this system and attempt to experimentally verify intriguing behaviour with a new kind of apparatus.

In section III, we present a mathematical description of the system followed by its implementation in a Matlab simulation in section IV. We use this simulation to examine the bifurcation and period-doubling of a system initially undergoing period-1 motion, as well as observe some more exotic behaviour. The preliminary experimental results are presented in section VII, and they form the foundation to an ongoing investigation into the topic. In subsequent work, we use a refined apparatus to accurately obtain experimental data and extend our investigation to include multiple driving frequencies.

II. Statement of Authorship

Research on this topic was proposed and supervised by Dr. Joel Miller, and carried out by Julian Ceddia. With the aid of Dr. Miller, the mathematical model presented in this paper was devised. Julian was responsible for writing the simulation in Matlab, as well as designing and constructing the experimental apparatus, and performing the experiment.

III. Modelling the System

In this section, we set up the equations governing our mathematical model of the system. The position of the table will be a prescribed function of time. The motion of the ball between bounces will be governed purely by gravity. The interaction of the two occurs only at the bounces, which are characterised by the coefficient of restitution.

Consider the oscillating table with a bouncing ball in Fig 1. The table's height, $y(t)$, can be described by the sum of sinusoids in Eq. (2.1). In this paper we only deal with $j = 1$.

$$y(t) = \sum_{i=1}^{j} A_i \sin(\omega_i t + \varphi_i) \tag{2.1}$$

The table's velocity is the given by

$$\dot{y}(t) = \sum_{i=1}^{j} A_i \omega_i \cos(\omega_i t + \varphi_i) \tag{2.2}$$

Eq. (2.3) is the parabolic path of the ball between bounces, where $(t - t_{n-1})$ is the time elapsed after the previous bounce and c_n is the collision height of the n^{th} bounce. u_n is the ball's rebound velocity, after the n^{th} bounce. Under these circumstances, $X(t)$ is the piecewise function made up of n bounces.

$$x_n(t) = c_{n-1} + (t - t_{n-1})u_{n-1} + \frac{1}{2}g(t - t_{n-1})^2 \tag{2.3}$$

$$X(t) = \begin{cases} x_1, & 0 < t < t_1 \\ \vdots & \vdots \\ x_n, & t_{n-1} < t < t_n \end{cases} \tag{2.4}$$

The coefficient of restitution is defined by the ratio of the relative velocities of the ball and table before and after a collision, Eq. (2.5) [7]. Here we denote the times immediately before and after the n^{th} collision as t_{n-} and t_{n+} by taking the limit $t \to t_n$ from either side, and express the ball's impact velocity as v_n.

$$e = -\frac{\dot{y}(t_{n+}) - \dot{X}(t_{n+})}{\dot{y}(t_{n-}) - \dot{X}(t_{n-})} = -\frac{\dot{y}(t_n) - u_n}{\dot{y}(t_n) - v_n} \tag{2.5}$$

If we assume the table is adequately rigid (i.e. $\dot{y}(t_{n-}) = \dot{y}(t_{n+}) = \dot{y}(t_n)$), such that it is undisturbed by the bounce of the ball, the ball's rebound velocity, u_n, immediately after the nth collision at time t_{n+} is then given by Eq. (2.6).

$$u_n = \dot{y}(t_n) + e(v_n - \dot{y}(t_n)) \tag{2.6}$$

We can find the height and time of the n^{th} bounce, if we assume some initial conditions about the ball's release and then equate Eq. (2.1) and (2.3).

$$c_{n-1} + (t - t_{n-1})u_{n-1} + \frac{1}{2}g(t - t_{n-1})^2 = A\sin(\omega t + \varphi) \tag{2.7}$$

A nondimensionalisation analysis of these equations can be found in the appendix. For the purposes of comparing simulation with experiment, dimensions were left in.

If we consider period-1 motion, we can recognise the restrictions imposed on the initial conditions of the system. For instance, for period-1 motion to occur, the ball must perpetually bounce on the table at particular point in the table's phase, as shown in Fig. 2.

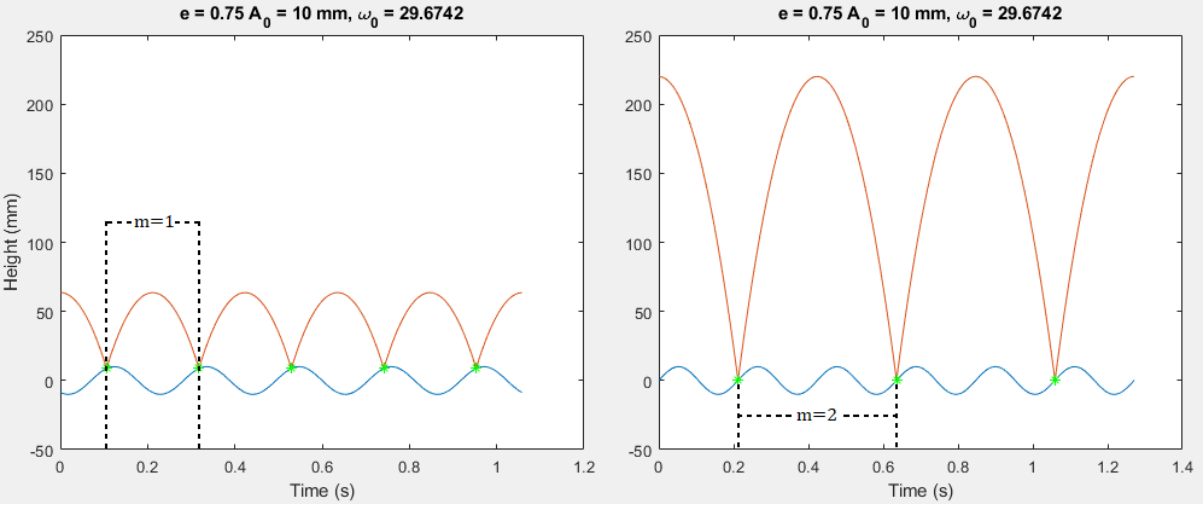

Fig 2 *– On the left, we have period-1 motion, where the ball (red) impacts the table (blue) every period (m=1). On the right, we have period-1 motion again, however the ball impacts the table every second period (m=2). 'm' is the number of periods skipped.*

In other words, the time between bounces, τ , must be an integer multiple of the table's period (i.e. $\tau = mT$). With the aid of Fig. 2, we also see that, due to the parabolic path of the ball, its impact speed and rebound speed must be same. Thus from Eq. (2.3), we can determine a suitable rebound velocity, u_n.

(3.1) $$u_n = \frac{\tau g}{2}$$

Substituting $\tau = mT$, where $T = \frac{2\pi}{\omega}$ gives

(3.2) $$u_n = \frac{m\pi g}{\omega}$$

Since $u_n = -v_n$, assuming that the first bounce occurs at $t_1 = 0$, Eq. 2.6 becomes

(3.3) $$u_n = A\omega\cos(\varphi)\frac{(1+e)}{(1-e)}$$

Substituting into Eq. (3.2) gives

(3.4) $$\cos(\varphi) = \frac{m\pi g}{A\omega^2}\frac{(1-e)}{(1+e)}$$

If Eq. (3.4) is satisfied, the system will, theoretically, exhibit period-1 motion, however demonstrating period-1 motion in practice requires that the solution be stable. It is therefore necessary to be able to quantify the stability of such a solution.

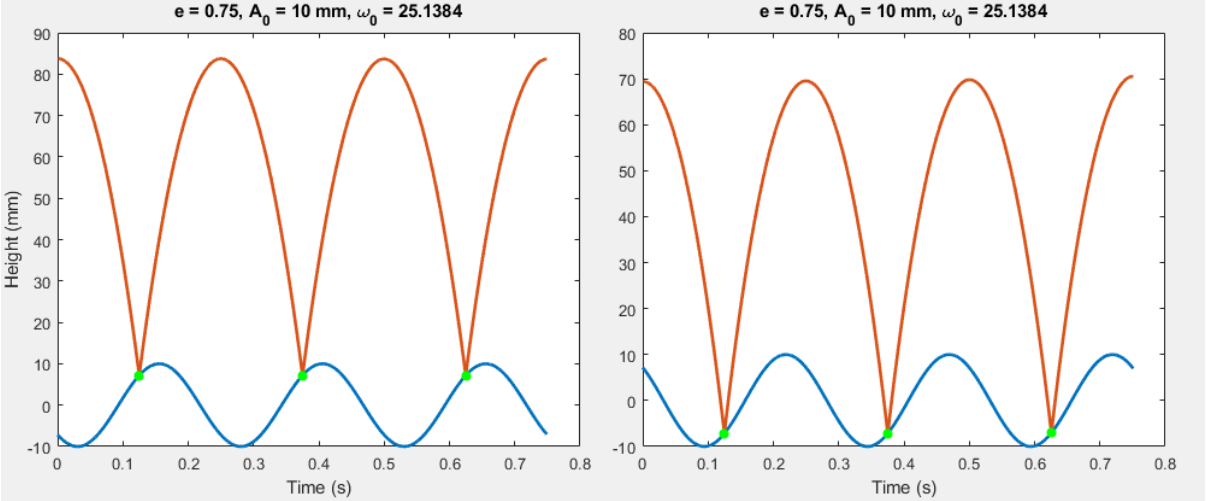

Fig 3 – *Stable (left) and unstable (right) period-1 motion. On the left, if the ball bounces slightly short of where it needs to, it will receive more energy from the table, making it travel slightly farther on the next bounce and visa-versa if it hits slightly later than it needs to. In this case, the ball eventually settles on a stable solution (the solution is an attracting fixed point). In the solution depicted on the right, the opposite is true. In this case the ball quickly diverges from its periodic motion (the solution is a repelling fixed point).*

Performing nondimensionalisation (see appendix) yields the reduced acceleration parameter, Γ, found in [3]. This parameter can be found in Eq. (3.4), and rewriting gives Eq. (3.6).

(3.5) $$\Gamma = \frac{A\omega^2}{\pi g}$$

(3.6) $$\Gamma = \frac{m}{\cos(\varphi)}\frac{(1-e)}{(1+e)}$$

As shown by Luck in [3], perturbation theory leads to an inequality that must be satisfied for stable periodic motion is given in Eq. (3.7).

(3.7) $L < \Gamma < U$ Period-1 stability [3]

(3.8) $L = m\frac{(1-e)}{(1+e)}$, Lower limit [3]

(3.9) $U = \sqrt{\left(\frac{m(1-e)}{(1+e)}\right)^2 + \left(\frac{2(1+e^2)}{\pi(1+e)^2}\right)^2}$, Upper limit [3]

The lower limit can be intuitively realised from Fig. 4, corresponding to $\varphi = 0$ in Eq. (3.6). From Fig. 4, we see that the ball is initially bouncing at an inflection point in the table's cycle. This inflection point corresponds to the table's maximum velocity, so if the ball bounces either side of it, it will lose energy. Thus, this period-1 solution is attracting from the $\varphi \geq 0$ side, and repelling from $\varphi < 0$ side. In this case, the bouncing of the ball is ephemeral, before a sticking solution is reached.

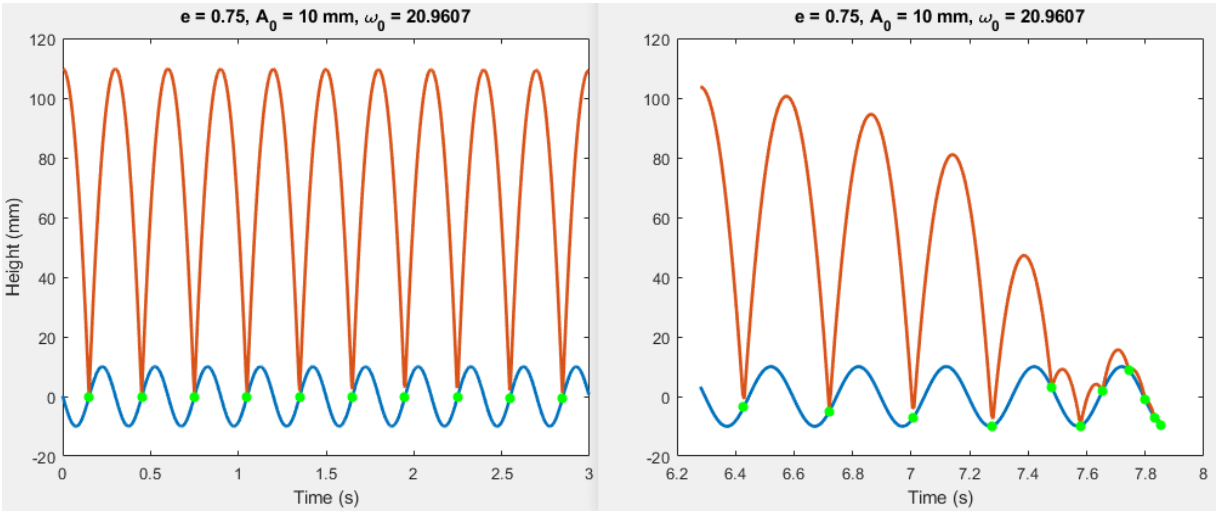

Fig 4 *– Bounces 1-10 (left) and 22-32 (right). Unstable period-1 motion – lower limit predicted by Eq. (3.8) for* $m = 1. \Gamma = L = 0.1428$.

The upper limit requires a little more insight to visualise conceptually. It emerges from the fact that a perturbed stable periodic solution oscillates around a fixed-point, where the fixed-point error diminishes with each oscillation. Once this upper limit, U, is surpassed, the oscillations no longer decay. Thus a period-doubling bifurcation occurs.

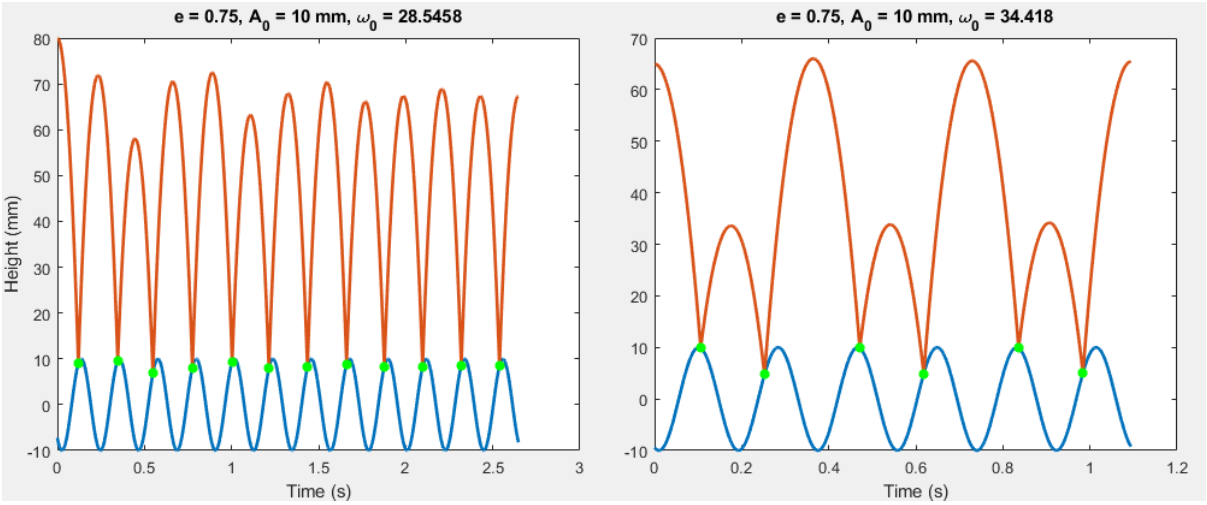

Fig 5 *– Oscillations around the stable period-1 fixed point,* $\Gamma < U$ (left). Period-doubling bifurcation as Γ exceeds the upper limit U (right).

IV. Simulation

The mathematical model in section III formed the basis for the simulation written in MATLAB. Unfortunately, solving Eq. (2.7) requires numeric approximations due to the bounces occurring at the intersection of a parabola and a sinusoid. MATLAB's built in 'vpasolve' function was able to give such approximations to 10 decimal places quickly, using a Newton type root search [8]. The results presented in this section are for $e = 0.75$. This chosen coefficient of restitution reflects that of the ball used in the experiment in section V.

Period-1 and Subsequent Period Doubling Bifurcation

Considering the case where Eq. (3.7) is satisfied, we take an arbitrary $m = 1$ instance of stable period-1 motion, and introduce a perturbation by increasing the ball's release height. We can confirm that the solution is attracting from the phase space diagram in Fig. 6, where the ball 'circles in' on the fixed-point.

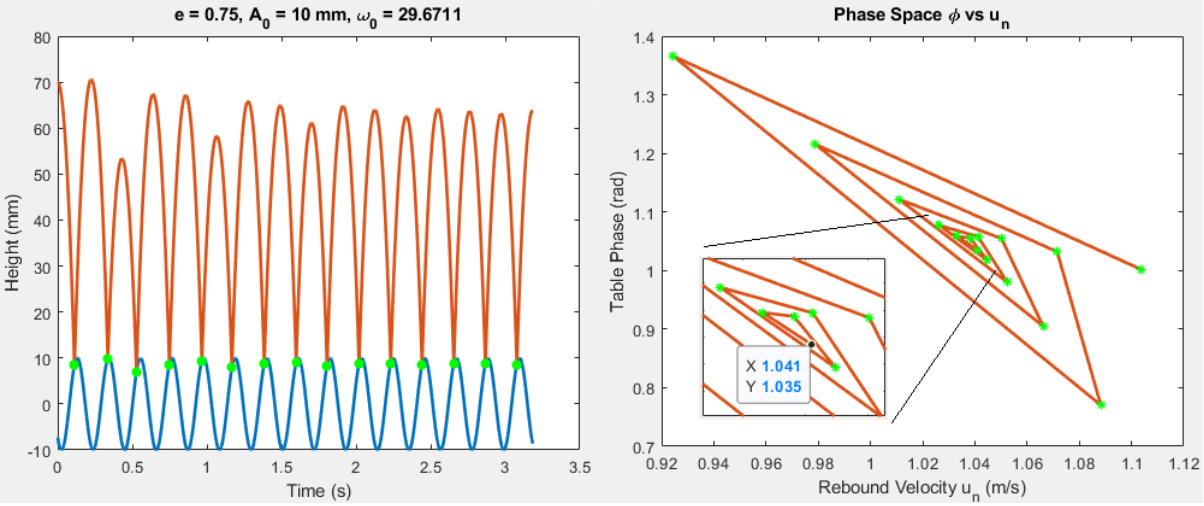

Fig 6 *– $\Gamma = 0.286$. A stable solution perturbed by increasing the drop height. The phase space diagram shows the system circling around the attracting point which is numerically calculated to be (1.037, 1.039).*

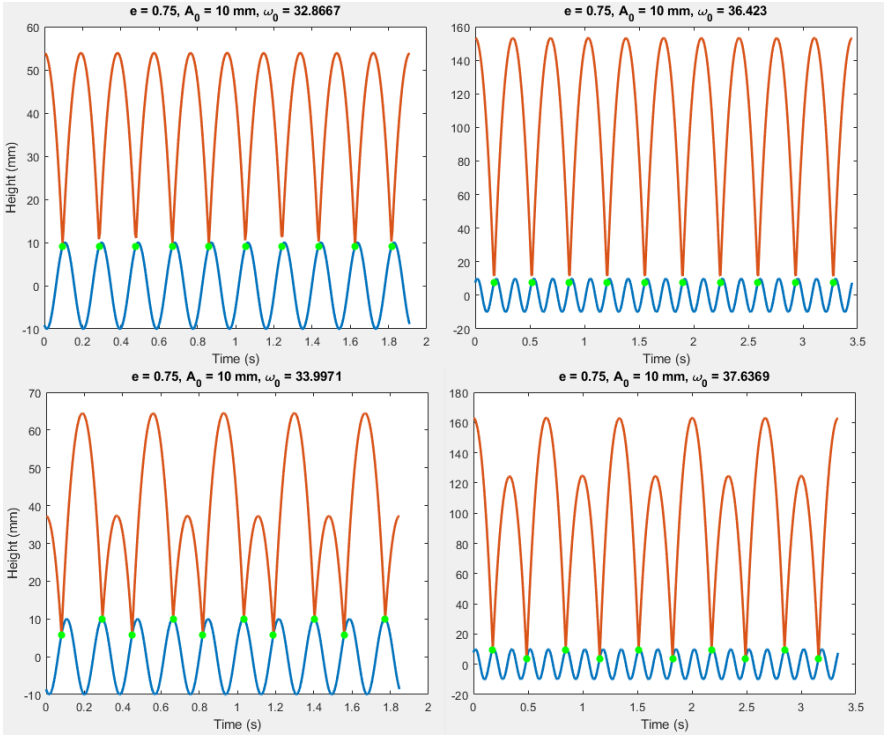

Fig 7 *– Period-doubling occurs when $\Gamma > U$. From top left to bottom right; $\Gamma = 0.351$, $\Gamma = 0.430$, $\Gamma = 0.375$, and $\Gamma = 0.470$*

As we move beyond the upper stability limit such that $\Gamma > U$, bifurcation occurs and we observe period-doubling. Fig. 7 above shows this for m=1 and m=2 cases. Note that for $m = 1, U = 0.355$ and for $m = 2, U = 0.433$.

If we continue to increase Γ, we can experimentally find subsequent bifurcation points. In Fig. 8, driving frequency (left) and driving amplitude (right) are increased while the resulting stable orbits are plotted. Corresponding bifurcation points from each figure occur at the same Γ value, revealing that the two bifurcation diagrams are essentially the same thing viewed from different perspectives – as nondimensionalisation implies.

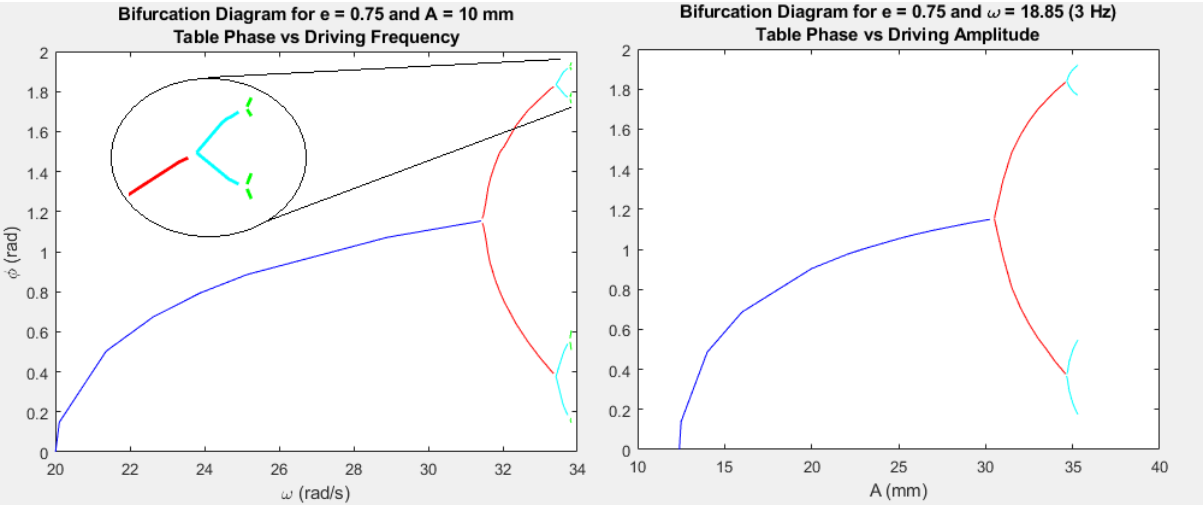

Fig. 8 – *Bifurcation diagrams for increasing table frequency (left) and amplitude (right). The first second bifurcation points each occur at* $\Gamma = 0.352$ *and* $\Gamma = 0.399$*, respectively, for both plots.*

Plotting the $m = 1$ limits from Eq. (3.8) and (3.9) shows the region where period-1 solutions are permitted. The first and second period-doubling bifurcations in Fig. 8 correspond to points 4 and 5 on the line $e = 0.75$ in Fig. 9.

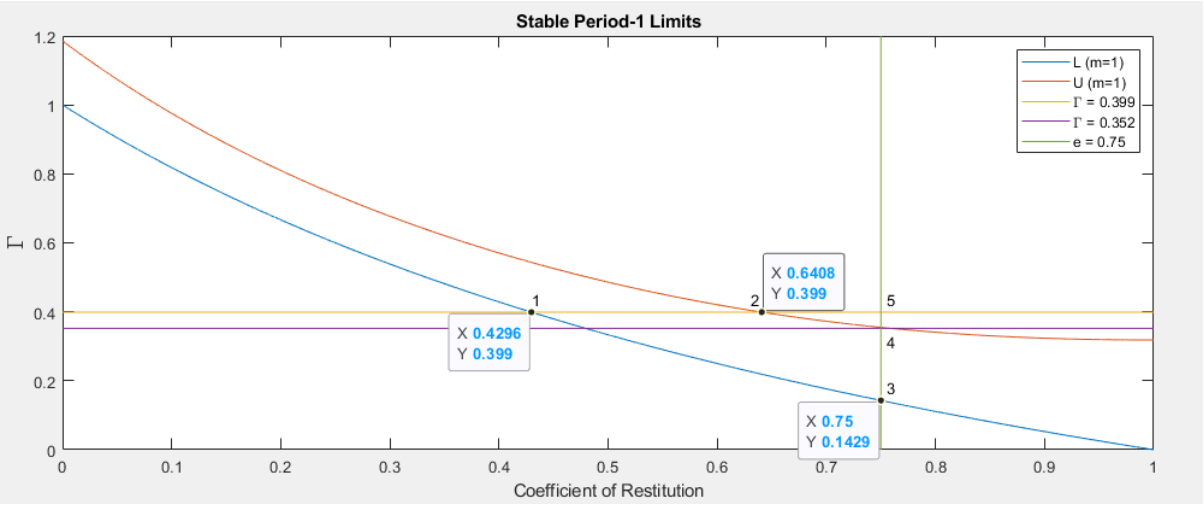

Fig. 9 – *Stable period-1 regions.* $e = 0.75$*, is marked apropos to the bifurcation diagrams above, and the line* $\Gamma = 0.399$ *to the bifurcation diagram in Fig. 10. The intersection of* $\Gamma = 0.352$ *and* $e = 0.75$ *is the occurrence of the first bifurcation point.*

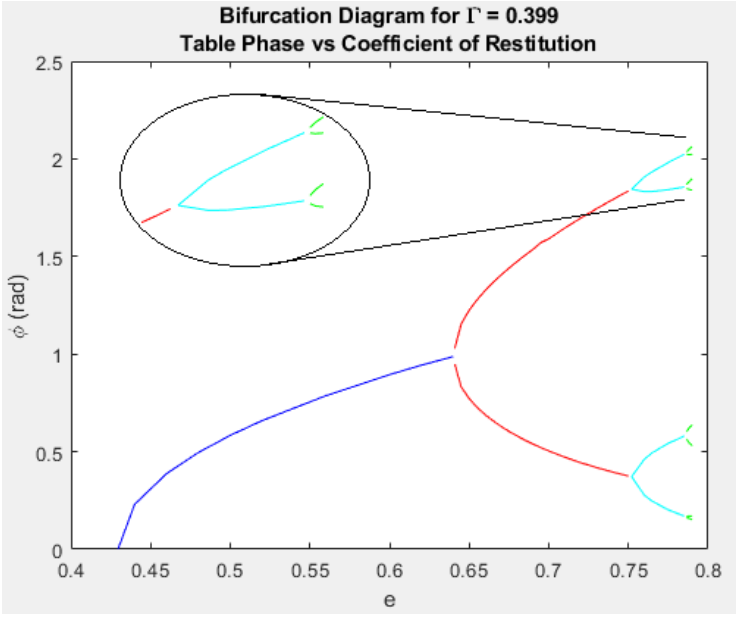

Fig. 10 *– Period-doubling bifurcation with constant* Γ*. The first and second bifurcation points correspond to points 2 and 3 in Fig. 9.*

Period-3 and Subsequent Period Doubling Bifurcation

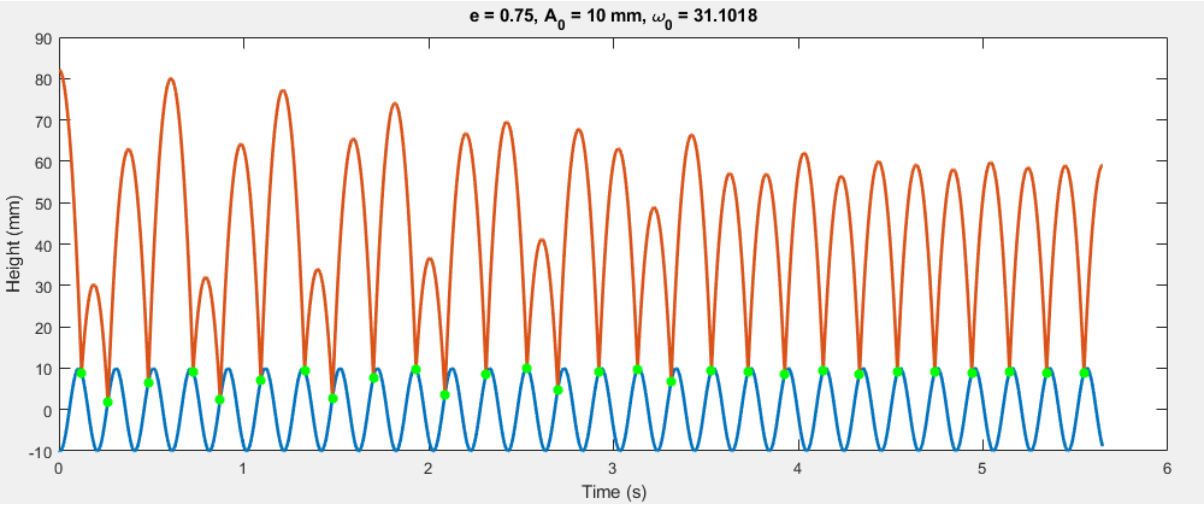

Fig. 11 *– Saddle point bifurcation for* $\Gamma = 0.314$ *– lower limit for period-3 motion. Period-3 motion decays into period-1. In the first 12 bounces, it is clear that each distinct peak in the period-3 sequence approaches the settling height, of around 58 mm, in quite a regular fashion.*

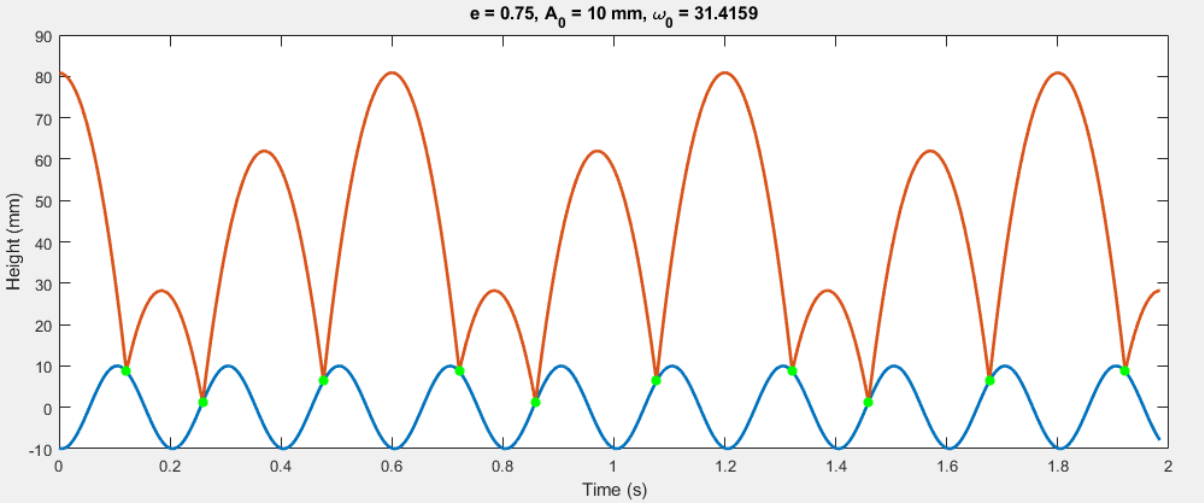

Fig. 12 *– $\Gamma = 0.320$, slightly above the lower limit for stable period-3 motion. This corresponds to the approximate location of the saddle point bifurcation in Fig. 13.*

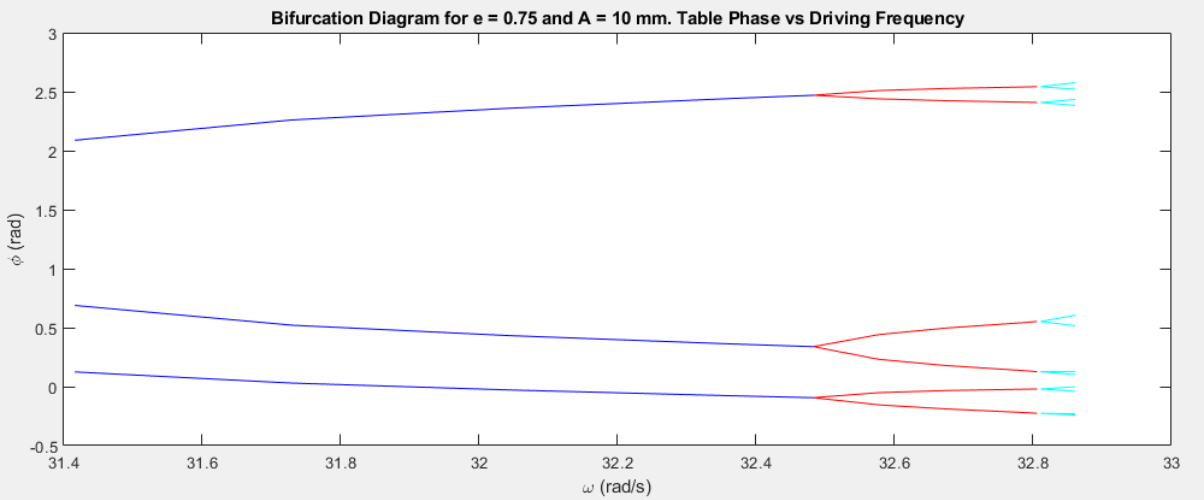

Fig. 13 *– Bifurcation diagram beginning with period-3 motion. The saddle point bifurcation is around $\Gamma = 0.320$. The period-doubling bifurcations occur at approx. $\Gamma = 0.3424$ and $\Gamma = 0.3493$.*

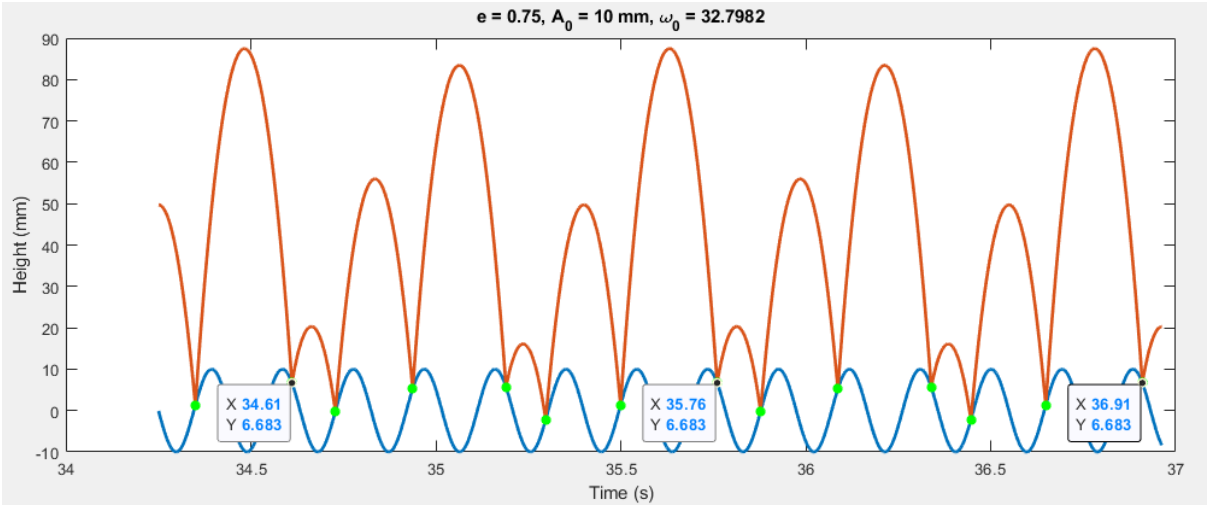

Fig. 14 *– $\Gamma = 0.3490$, an example of stable period-6 motion.*

V. Experiment

In previous work, experiments have typically been carried out with the use of a loudspeaker and a ball-bearing. This means they are limited to relatively high frequencies (greater than 60 Hz [4,5]). Our approach allows us to examine the same behaviour at much lower frequencies, ranging from 0 Hz to 12 Hz.

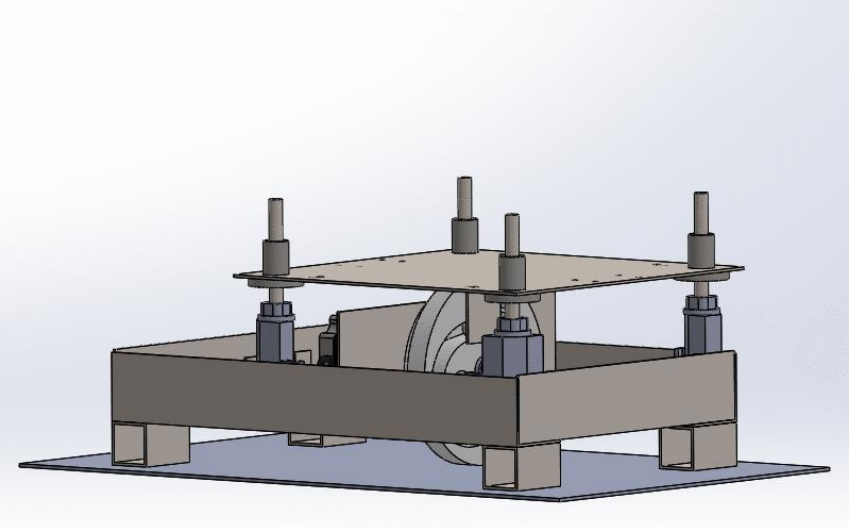

Fig. 15: *The plate has a linear bearing at each vertex for alignment. A bearing attached to the vertical section rides in the groove of a CAM. As the CAM rotates, the table's height tracks the radius of the groove. A high torque stepper motor with 0.45º step size drives the CAM.*

The data acquisition process uses a high-speed camera (240 fps) to capture the moment the ball bounces on the table. The ruled lines allow for a rough measurement of the table's phase at the time of the bounce.

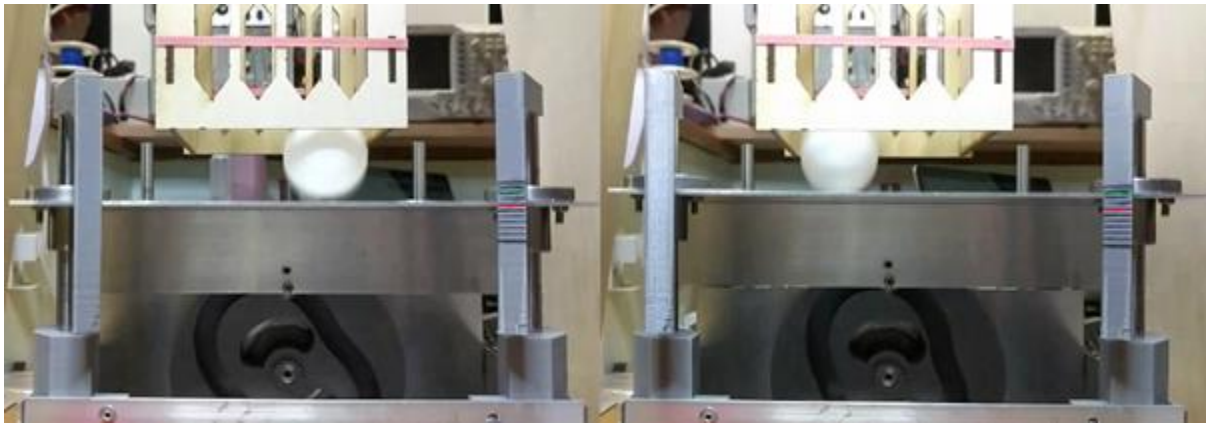

Fig. 16 – *Period-1 motion for* $\Gamma = 0.157$ *(left) and* $\Gamma = 0.273$ *(right). The red and green lines (3mm and 8mm) indicate the table's phase at each bounce is approx.* $\varphi = 0.3$ *and* $\varphi = 0.9$*. These values roughly agree with Fig. 8 corresponding to* $\omega = 20.9$ *and* $\omega = 27.6$ *where* $\varphi = 0.39$ *and* $\varphi = 1.01$ *respectively.*

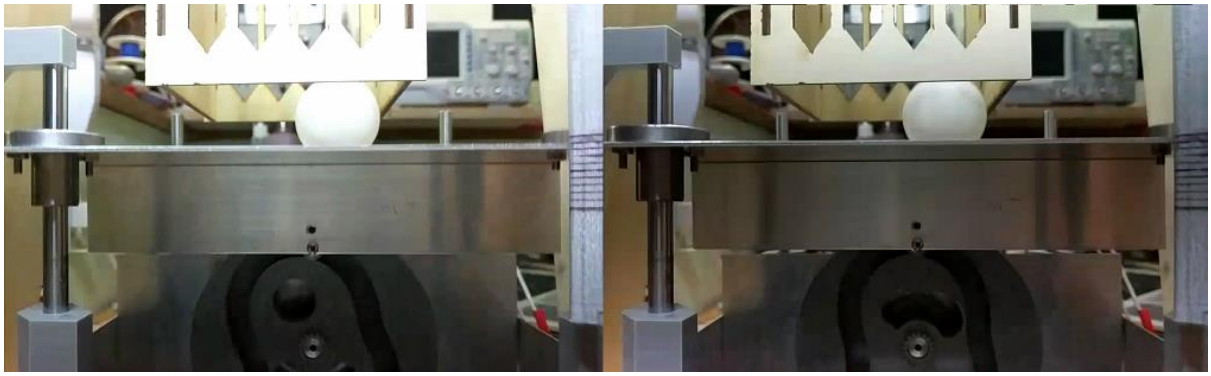

Fig 17 *– Period-2 motion with* $\Gamma = 0.358$*. These two frames show successive bounces that are representative of other bounces in the high-speed footage. On the left, the table's height is approx. 8 mm. On the right, the table's height is approx. 10 mm. These correspond to* $\varphi = 0.9$ *and* $\varphi = 1.5$*.*

For $\Gamma = 0.358$ in Fig. 17, the points of impact, according to Fig. 8 should be $\varphi = 0.94$ and $\varphi = 1.32$. The larger error in the latter is due to the fact that the ball is bouncing close to a peak in the table's oscillation. This amplifies the uncertainty when calculating the table's phase; close to the peak, very small changes in table height cause relatively large changes in phase.

VI. Discussion

The mathematical model presented in this paper can only predict the first period-doubling bifurcation point for period-1 motion. All others were found numerically, by adjusting the appropriate simulation parameter (frequency, amplitude, or coefficient of restitution), and then allowing the simulation to run until equilibrium was reached. In cases where the system was in a state impending a bifurcation point, the settling time to equilibrium was protracted. This is the primary source of uncertainty in the location of bifurcation points; equilibrium solutions might be dissembled and prematurely declared.

In section V we looked at the period-doubling bifurcation of both period-1 and period-3 motion. Period-doubling from $n = 1$ has been studied extensively, with findings in agreement to those presented here. Period-doubling from $n = 3$ however, has, to the extent of our knowledge, not been covered so thoroughly in the context of this topic. It was alluring to find a stable case of $n = 3$ in simulation. As shown in section V, the stable regions for period-3 overlap with period-1 and period-2 (i.e. for a single value of Γ, multiple stable orbits exist). According to a 1975 paper by Li & Yorke [9], the presence of period-3 in a one-dimensional system implies the existence of all other degrees of periodic motion. It remains an open question as to whether this is the case for our two-dimensional system (2D in the sense that a bounce is characterised by two parameters φ and v).

The experimental data acquisition technique used here needs substantial improvement to make reliable and meaningful measurements that are worthy of comparison to expectations set by simulation. Enhancements to the apparatus are ongoing. The table's phase can be accurately measured with a laser reflecting off the surface of the table to a detector, and bounces of the ball can be detected with a microphone. More work needs to be done so the two sets of data can be collected simultaneously, enabling them to be overlayed to produce a meaningful plot, comparable to simulation.

VIII. Conclusion

Simulations carried out in this research have highlighted the depth and complexity exhibited by a bouncing ball on an oscillating table. We have shown successive period-doubling bifurcations occurring for $n = 1$ and $n = 3$ stable orbits, as well as bifurcations in the context of changing the coefficient of restitution of the system. It was pleasing to have some experimental verification of $n = 1$ and $n = 2$ periodic motion using the apparatus in section V, and valuable to learn about the shortcomings of the data acquisition techniques used in this approach. Ultimately, this research has allowed us to explore, and become familiar with this dynamical system; it has provided the foundation required to pursue research on this topic in a novel and exciting way that, we hope, will lead to a positive contribution.

VII. References

[1] Luo, A.C.J. & Han, R.P.S. Nonlinear Dyn (1996).

[2] Holmes, P. J., 'The dynamics of repeated impacts with a sinusoidally vibrating table', Journal of Sound and Vibration 84, 1982, 173-189.

[3] Luck, Jean-Marc & Mehta, Anita. (1993). Bouncing ball with a finite restitution: Chattering, locking, and chaos. Physical review. E, Statistical physics, plasmas, fluids, and related interdisciplinary topics. 48. 3988-3997.

[4] Period doubling boundaries of a bouncing ball N.B. Tufillaro, T.M. Mello, Y.M. Choi, A.M. Albano J. Phys. France 47 (9) 1477-1482 (1986)

[5] Jumping particle model. A study of the phase space of a non-linear dynamical system below its transition to chaos Pi. Pierański, Z. Kowalik, M. Franaszek J. Phys. France 46 (5) 681-686 (1985)

[6] Effect of collision duration on the chaotic dynamics of a ball bouncing on a vertically vibrating plate. Z.H. Jiang, Z.J. Liang, A.C. Wu, R.H. Zheng. Physica A 494 380-388 (2018)

[7] M.Heckel, A.Glielmo, N.Gunkelmann, T.Poschel. (2016). Can we obtain the coefficient of restitution from the sound of a bouncing ball?: Physical review. E 93, 032-901

[8] Walter Roberson, Mathworks – MATLAB Answers (online) au.mathworks.com/matlabcentral/answers/298048

[9] Tien-Yien Li, James A. Yorke. (1975) Period Three Implies Chaos: The American Mathematical Monthly, Vol. 82, No. 10.

VIII. Appendix

A.1 Nondimensionalisation

We start by measuring time in units of the table's oscillation period $T = \frac{2\pi}{\omega}$

(A.1) $$\hat{t} = \frac{\omega t}{2\pi}$$

Length can be rescaled to have units of $\frac{4\pi^2 g}{\omega^2}$ so the table's amplitude becomes

(A.2) $$\hat{A} = \frac{A\omega^2}{4\pi^2 g}$$

Recall that the table's motion is described by

(2.1) $$y(t) = A\sin(\omega t + \varphi)$$

From (2.1), applying nondimensionalisation, the table's we get

(A.3) $$\hat{y}(\hat{t}) = \frac{\Gamma}{4\pi}\sin(2\pi\hat{t} + \varphi), \text{ where } \Gamma \text{ is given by}$$

(A.4) $$\Gamma = \frac{A\omega^2}{\pi g}$$

This nondimensionalisation reduces the system to two parameters, Γ and $\hat{t}$, combining amplitude and oscillation frequency.

A.2 Cam Design

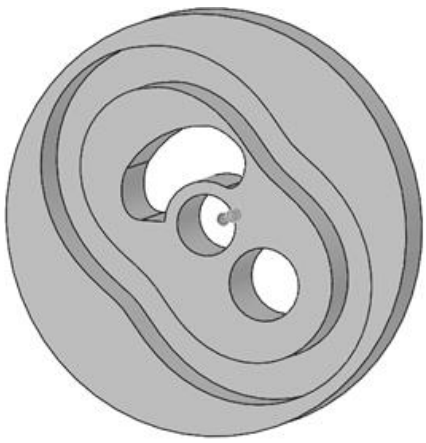

Fig A.1: *A balanced CAM with two periods of a single frequency. $A = 10$ mm*

Fig. A.1 shows the CAD drawing of the 3D printed CAM used in the apparatus. Two periods of a single frequency are encoded in the bearing track. This design drastically increases the size of the CAM, however relieves stress on the motor by halving its rotational velocity. A similar method has been used to design a CAM with two frequencies encoded into the track, so that the table can oscillate at the sum of two sinusoids.